Selective PQQPFPQQ gluten epitope chemical sensor with a molecularly imprinted polymer recognition unit and an extended-gate field-effect transistor transduction unit

Zofia Iskierko,[1]* Piyush S. Sharma,[2] Krzysztof R. Noworyta,[2] Pawel Borowicz,[2] Maciej Cieplak,[2] Wlodzimierz Kutner,[2,3]* and Alessandra Maria Bossi[1]*

[1]Department of Biotechnology, University of Verona, Strada Le Grazie 15, 37134 Verona, Italy
[2]Institute of Physical Chemistry, Polish Academy of Sciences (IPC PAS), Kasprzaka 44/52, 01-224 Warsaw, Poland
[3]Faculty of Mathematics and Natural Sciences, School of Science, Cardinal Stefan Wyszynski University in Warsaw

ABSTRACT: A molecularly imprinted polymer (MIP) recognition system was devised for selective detection and determination of one of the immunogenic gluten 8-mer epitope, PQQPFPQQ. For that purpose, a thin MIP film was designed and fabricated, guided by DFT calculations, and then synthesized to serve as the chemosensor recognition unit. For preparation of this unit, *bis*(bithiophene)-based cross-linking and functional monomers were used. An extended-gate field-effect transistor (EG-FET) served as the transduction unit. The EG-FET gate area was coated with the PQQPFPQQ-templated MIP film, by electropolymerization, to result in a complete chemosensor. Both templated and template-extracted MIP films as well as non-imprinted polymer (NIP) films were characterized by XPS to demonstrate template incorporation in the MIP, and then its extraction. The devised chemosensor rapidly and selectively responded to the gluten epitope analyte. It discriminated between the 8-mer analyte and another peptide of the same number of amino acids but with mismatched two of them (PQQ**Q**FP**P**Q). The chemosensor was validated with respect to both the PQQPFPQQ analyte and a real gluten extract from semolina flour. It was capable to determine the PQQPFPQQ analyte in the concentration range of 0.5 to 45 ppm with the limit of detection, LOD = 0.11 ppm. Moreover, it was capable to determine gluten in real samples in the concentration range of 4 to 25 ppm with LOD = 4 ppm, which is a value sufficient for discriminating between gluten-free and non-(gluten free) food products. The gluten content in semolina flour determined with the chemosensor well correlated with that determined with a commercial ELISA gluten kit. Langmuir, Freundlich, and Langmuir-Freundlich sorption isotherms were fitted to the epitope sorption experimental data. The sorption parameters determined from these isotherms indicated that the imprinted cavities were quite homogeneous and that the epitope analyte was chemisorbed in these cavities.

Food allergies are becoming increasingly common nowadays. Among others, gluten intolerance is the second most common food allergy, just after lactose intolerance. Gluten is the allergen that triggers the autoimmune reactions in humans suffering from celiac sprue (CS). In Europe, CS affects ~1-2% of population generating direct annual costs of ~3 billion EUR for diagnosis and treatments.[1]

Because CS is a chronic illness, gluten uptake remains dangerous for the entire lifespan of patients with CS diagnosed. Indeed, the intestinal villi of CS patients are being damaged as long as gluten is present in their diet.[2,3] Atrophic villi structure badly affects assimilation of food components, and, in effect, can be the foreground for other severe diseases including cancer.

At the present medicine advancement, there is no effective cure for CS. Therefore, patients suffering from CS must stick to a rigorous gluten-free diet. Gluten-free food should go through quality testing in accredited laboratories, in order to be certified with the symbol of the crossed ear, internationally acknowledged to indicate gluten-free food product that contains less than 20 mg of gluten ppper 1 kg of the whole food sample. The current gluten tests, mainly involving immunodetection, such as immunoenzymatic assays,[4] need a qualified personnel, sophisticated equipment, and expensive reagents. Therefore, a simple and portable gluten sensor is of utmost importance for gluten-intolerant and CS suffering patients.

Indeed, some attempts are being undertaken to devise a fast performing, easy to use, and reliable chemosensor for gluten detection and determination. For instance, an electrochemical gluten sensor was recently devised.[5] Direct electrochemical oxidation of gluten amino acids was exploited in it to determine the gluten level. This chemosensor was referred to as a simple and cheap device "ready to evaluate the purity of gluten-free products specially to ensure a safe diet for celiac patients". As the transduction electroanalytical technique, differential pulse voltammetry (DPV) was applied. A specially processed graphite pencil electrode (PGE) was used as the working electrode (recognition unit).[6]

Chemical gluten recognition is not straightforward because the molecular structure of gluten is complex.[7,8] Detecting the immunogenic part of the gluten molecule, instead of the whole gluten molecule is already well established.[9] Particular attention has been paid to the 33-mer peptide from α2-gliadin, widely described as the most important CS-immunogenic epitope of gluten.[4] However, this 33-mer peptide is not shared by all gluten sources, e.g., it is absent in barley. Therefore, many other immunogenic epitopes of gluten are proposed in literature.[10-12] For the purpose of the present research, we chose the PQQPFPQQ epitope because of its presence in wheat, rye, and barley.[13,14]

Molecularly imprinted polymers (MIPs) are synthetized from functional and cross-linking monomers, which are co-polymerized in solution in the presence of a template.[15,16] The template removal from the MIP thus prepared results in emptying the imprinted molecular cavities. The cavity shape, size, and orientation of its recognition sites generated that way correspond to the shape, size, and orientation of binding sites of the template molecule. MIPs, particularly those prepared in the form of thin films, are successfully integrated with different transducers for fabrication of selective chemosensing systems used to determine different analytes.[17-19] The desired MIP selectivity is gained by careful designing of the molecular cavities. In these cavities, different recognition sites are generated in a well-defined manner so to provide a proper stereochemical microenvironment for the reversible binding of the target analyte molecules. Many reviews as well as original research articles describe preparation and application of selective MIP-based chemosensors.[17,19-22]

Here, we propose a thin film of a conducting polymer molecularly imprinted with a gluten epitope of the PQQPFPQQ amino acid sequence as the artificial recognition unit of a gluten-selective MIP chemosensor. The size of the chosen epitope seems reasonable for the purpose of imprinting. Imprinting of an epitope of a similar number of amino acids has already been successfully demonstrated for protein recognition.[23-25]

To our best knowledge, no EG-FET chemosensor has so far been devised with an MIP recognition unit for gluten determination. The combination of FETs with MIPs provides high sensitivity and selectivity,[26] which is so much demanded for analytical determinations. The results of our proposed method were compared with those obtained using a commercially available gluten recognition kit based on immunodetection. Herein, both methods were used to determine gluten in the extract from natural semolina flour.

EXPERIMENTAL SECTION

Reagents

Synthetic details on preparation of the functional monomers, vis., *p*-bis(2,2'-bithien-5-yl)methylbenzoic acid 2,2-(cytosin-1-yl)ethyl *p-bis*(2,2'-bithien-5-yl)methylbenzolate 3 and the cross-linking monomer, 2,4,5,2',4',5'-hexa(thiophen-2-yl)-3,3'-bithiophene 4, used in the present work are described elsewhere.[27-29] All synthesized monomers were purified by HPLC before use. Purified gluten epitopes, PQQPFPQQ 1 (Scheme S1a in Supporting Information), and PQQ**Q**FP**P**Q were purchased from GL Biochem (Shanghai, China). Anhydrous solvents, vis. acetonitrile and toluene, as well as gluten from wheat were procured from Sigma-Aldrich. Electrochemical grade tetrabutylammonium perchlorate, $(TBA)ClO_4$, was purchased from Fluka. The isopropanol solvent was obtained from CHEMPUR. The MES buffer (>99% for biochemistry) was procured from Roth. The AgraQuant® Gluten G12 ELISA kit was purchased from Romer Labs. The gluten extract from semolina flour was prepared according to the Romer Labs procedure.

Instrumentation and procedures

Structure of the pre-polymerization complex was computationally optimized using the density functional theory (DFT) at the B3LYP level with the 3–21G* basis set, all implemented in the Gaussian 2009 software package.[30]

Polymer films were deposited on Au-glass slides (size 7×21 mm). These slides were prepared in the Institute of Electronic Materials Technology (Warsaw, Poland) by sputtering a thin (100 nm) Au layer over a thin (15 nm) Ti underlayer. These slides were used as supports for deposition of polymer films, and then used for further investigations, i.e., the atomic force microscopy (AFM), X-ray photoelectron spectroscopy (XPS), and polarization-modulation infrared reflection-absorption spectroscopy (PM-IRRAS) studies. Before each film deposition, Au-glass slides were cleaned with isopropanol in an ultrasonicator (160 W power IS-3R of InterSonic, Olsztyn, Poland) for 30 min. Moreover, Au-glass slides coated with MIP films were used as extended gates of extended-gate field-effect transistor (EG-FET) chemosensing systems.

An AUTOLAB computerized electrochemistry system of Eco Chemie, equipped with the expansion card of the PGSTAT 12 potentiostat, and controlled by GPES 4.9 software of the same manufacturer, was used for deposition of thin polymer films.

XPS spectra were recorded on a PHI 5000 VersaProbe™ (ULVC-PHI) scanning ESCA microprobe using monochromatic Al Kα radiation ($h\nu$ = 1486.4 eV). The XPS data were generated by a 100-μm diameter X-ray beam and collected from 250-μm^2 irradiated area. High-resolution (HR) XPS spectra were collected with a hemispherical analyzer at the pass energy of 23.5 eV, energy step of 0.1 eV, and photoelectron take off angle of 45° with respect to the surface plane. CASA XPS software was used to evaluate the XPS data. The background was subtracted using the Shirley method and peaks were fitted using the mixed Gaussian-Lorentzian method. Binding energy of the Au $4f_{7/2}$ peak (*BE* = 84.0 eV) was chosen as the internal reference.

AFM topography and nanomechanical property images were recorded using Multimode 8 microscope of Bruker equipped with a Nanoscope V controller operating in the PeakForce QNM mode. Nanoscope v.8.15 software was used for data acquisition and analysis. An RTESP silicon tip on the silicon cantilever with the spring constant of 42 $N\ m^{-1}$ was used for all experiments. Reduced Young's modulus was calculated from the force curves recorded

using the DMT model. For determining average film thickness, some parts of the films were carefully removed in few different places from the electrode surface, i.e., scratched with a Teflon™ spatula, under an optical microscope. Subsequently, these scratches were imaged with AFM. Then, heights of the resulting steps were measured by averaging the number of points on both sides of the step (sufficiently far from its partially detached front). The difference of the average values of points on the step and at its foot determined the height of the step. Finally, step heights measured for different scratches were averaged to determine an average value of film thickness.

A Keithley 2636A (1 fA, 10 A pulse) Dual-channel SourceMeter along with an EG-FET system of CD4007UB metal-oxide semiconductor field-effect transistor (MOSFET) was applied for measuring transistor characteristics necessary for PQQPFPQQ epitope determination. The EG-FET is a modified form of a MOSFET, in which the gate is extended outside of the transistor.[31-33] The MOSFET characteristics were taken under stagnant-solution conditions using a conical glass electrochemical minicell filled with 1 mL of 0.5 mM MES buffer (pH=6.2). The MIP film coated working electrode (gate) was mounted parallel to the Pt grid reference electrode. Distance between these electrodes was kept constant at ~10 mm.

Infrared (IR) spectra were measured with a Vertex 80 v Fourier Transform IR (FTIR) computer controlled Bruker spectrophotometer equipped with Opus 6.5 software of the same manufacturer. In order to record IR spectra for thin polymer films deposited on Au-glass slides, the PMA50 module was used. This module enables carrying out PM IRRAS measurements. Spectra were recorded with 2 cm^{-1} resolutions. For each spectrum, 1024 scans were recorded. The spectra were analyzed with SPESCA software.[34]

Deposition of a thin film of a polymer, molecularly imprinted with PQQPFPQQ, on an Au-glass slide electrode surface

The PQQPFPQQ-templated thin MIP films were simultaneously prepared and deposited on Au-glass slide electrodes using potentiodynamic electropolymerization. For that, the potential was cycled five times between 0 and 1.25 V vs. Ag/AgCl pseudo-reference electrode at a potential scan rate of 50 mV s^{-1}. An acetonitrile-toluene solvent mixture of the 1 : 9 volume ratio was used. For preparation of solutions for electropolymerization, the PQQPFPQQ template along with functional monomers **2** and **3** were dissolved in this mixture. DFT calculations suggested the 1 : 2 : 1 optimum molar ratio of the template to the functional monomer **2** and **3**, respectively. Moreover, the cross-linking monomer **4** at the template-to-monomer molar ratio of 1 : 1 was used to generate in the MIP molecular cavities accessible for the analyte molecules. Solution conductivity was afforded by a 0.1 M $(TBA)ClO_4$ supporting electrolyte. After deposition, the MIP film was rinsed with abundant acetonitrile to remove excess of the supporting electrolyte and non-polymerized monomers. The PQQPFPQQ template was then extracted from the film by liquid-solid extraction with the 10 mM NaOH and ethanol mixture at the volume ratio of 1 : 2, at room temperature, for 3 h. A control film of non-imprinted polymer (NIP) was deposited from the template-free solution using the same electropolymerization procedure.

Results and discussion

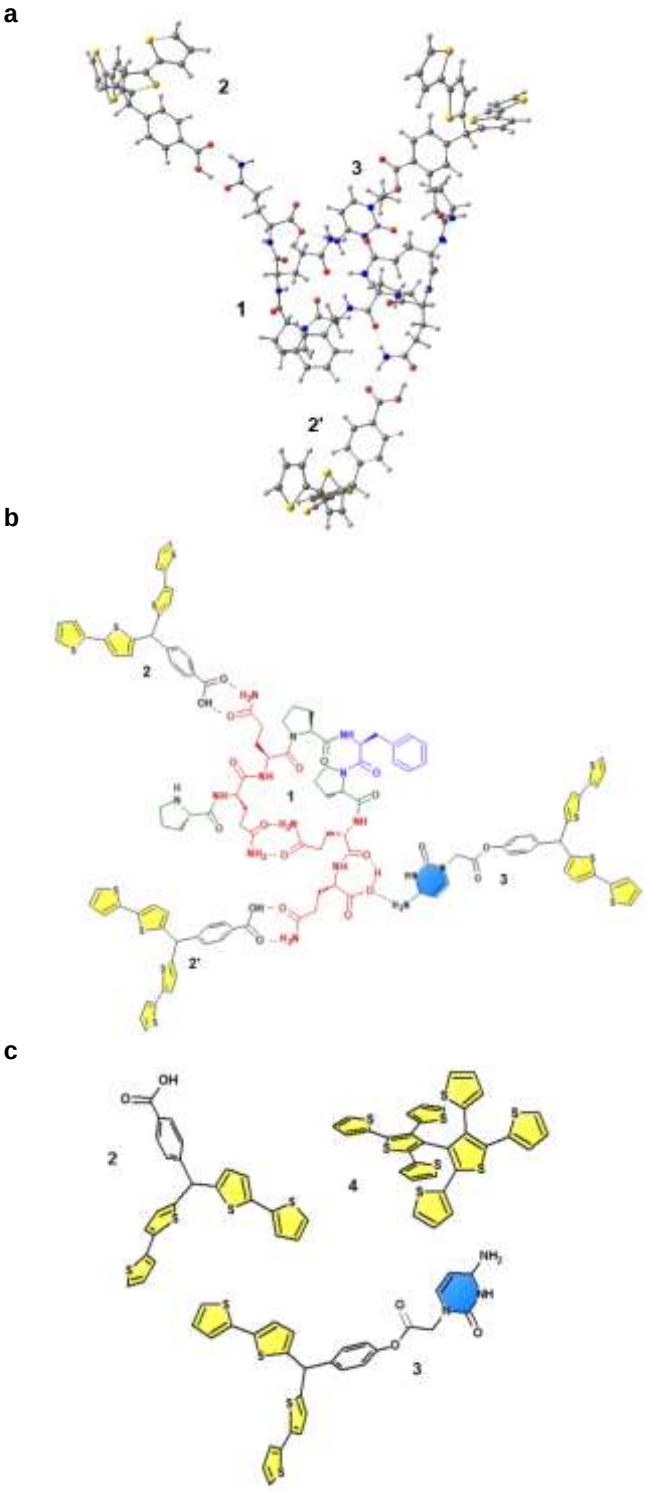

Scheme 1. (a) The B3LYP/3-21G* optimized structure of the pre-polymerization complex of the PQQPFPQQ **1** template with two molecules of **2** and one molecule of **3** functional monomers, (b) structural formula of this pre-polymerization complex, and (c) structural formulas of *p-bis*(2,2'-bithien-5-yl)methylbenzoic acid **2**, 2-(cytosin-1-yl)ethyl *p-bis*(2,2'-bithien-5-yl)methylbenzolate **3** functional monomers, and 2,4,5,2',4',5'-*hexa*(thiophen-2-yl)-3,3'-bithiophene **4** cross-linking monomer.

Selection of monomers bearing chemical functionalities complementary to the template/analyte binding sites is pivotal for the formation of stable pre-polymerization complexes in solution, ultimately resulting in well-defined molecular cavities in the polymer matrix. The formation of these complexes and appropriate monomer selection can be optimized by quantum chemistry calculations.

Table 1. The Gibbs free energy change (ΔG) values calculated for formation of pre-polymerization complexes of template **1** with the chosen monomers **2** and **3** at different molar ratios and in different media.

1 : 2 : 3 molar ratio	**Medium**	**DFT level/basis set**	**ΔG, kJ mol^{-1}**
1 : 1 : 0	vacuum	B3LYP/3-21G*	-101.86
1 : 2 : 0	vacuum	B3LYP/3-21G*	-289.45
1 : 0 : 1	vacuum	B3LYP/3-21G*	-105.63
1 : 1 : 1	vacuum	B3LYP/3-21G*	-210.92
1 : 2 : 1	**vacuum**	**B3LYP/3-21G***	**-333.88**
1 : 2 : 1	**toluene**	**B3LYP/3-21G***	**-302.66**

Here, changes of the Gibbs free energy (ΔG) corresponding to the formation of the complex of PQQPFPQQ with different functional monomers were DFT calculated. The higher the negative ΔG value, the higher is the stability of the pre-polymerization complex formed. Several different functional monomers with different functionalities were tested for finding the one most suitable. Structural formulas of different functional monomers used for computer modeling are shown in Scheme S2 in Supporting Information and the respective ΔG values calculated are summarized in Table S1 in Supporting Information. The preliminary screening step indicated that functional monomers **2** and **3** formed the most stable complexes. Table 1 summarizes the calculated ΔG values corresponding to formation of pre-polymerization complexes with the chosen monomers **2** and **3** at different molar ratios and in different media.

Scheme 1a shows the DFT optimized structure of the pre-polymerization complex revealing possible multi-point interactions between two molecules of functional monomer **2**, one molecule of functional monomer **3** and the PQQPFPQQ **1** template, in vacuum. In the structure-optimized complex, –COOH groups of **2** and –$CONH_2$ groups of glutamine components (in bold in PQ**Q**PFPQ**Q**) interact with the template molecule. Moreover, the cytosine moiety of **3** interacts with the PQQPFPQQ template by multi-point hydrogen bonding. The calculated negative value of ΔG was high, both for complexation in vacuum and in toluene (Table 1), which was the main solvent in the following polymerization procedure.

Figure 1 shows the current-potential curves of potentiodynamic electropolymerization of functional monomers **2** and **3** in the presence of the PQQPFPQQ **1** template and the cross-linking monomer **4**, thus resulting in deposition of an MIP film on the Pt disk electrode. The anodic peak at ~1.0 V vs. Ag/AgCl pseudo-reference electrode developed in the first cycle was assigned to irreversible electro-oxidation of the *bis*(bithiophene) moieties of the monomers. During the electro-oxidation, a radical cation is formed.[35] In the subsequent cycles the peak increased indicating formation of a conducting MIP film.

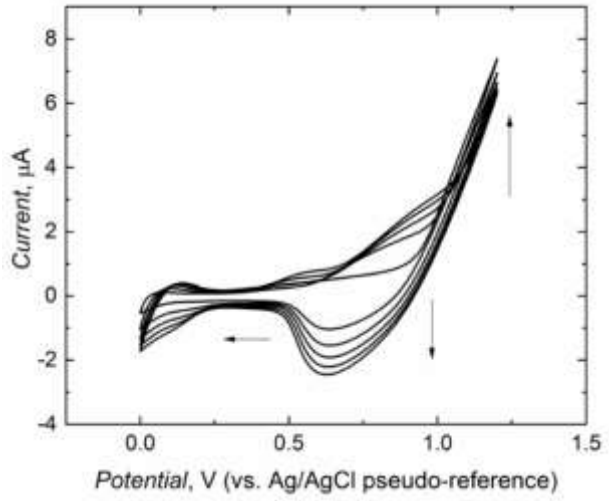

Figure 1. The current-potential curves for MIP-PQQPFPQQ film deposition by potentiodynamic electropolymerization on the 1-mm diameter Pt disk electrode in 0.1 mM **1** 0.2 mM **2**, 0.1 mM **3**, 0.1 mM **4**, and 0.1 M (TBA)ClO_4 in the toluene-to-acetonitrile solvent mixture of the 9 : 1 volume ratio. A potential scan rate was 50 mV s^{-1}.

Subsequently, the template was extracted with the 10 mM NaOH and ethanol mixture at the volume ratio of 1 : 2, so to disrupt both the electrostatic and hydrophobic interactions (selected properties calculated for the PQQPFPQQ epitope are listed in Scheme S1b in Supporting Information). The template extraction was monitored for 3 h. The template-extracted MIP and NIP films were then characterized by XPS to determine surface elemental composition of the films as well as to confirm the efficiency of template imprinting, and then extracting. Figure 2 shows the nitrogen content, determined with HR XPS. Before the extraction, the nitrogen content in the MIP film was 5.94 atomic % and it decreased to 3.26 % after the first 2 h of extraction. After additional 1 h of extraction the nitrogen content decreased to 2.86%. Extraction time further extending did not result in appreciable nitrogen content changes. Therefore, the total effective extraction time was

set at 3 h. The nitrogen content estimated for the NIP film before extraction was ~2 atomic %.

PM IRRAS measurements on the MIP film before and after template extraction were performed to confirm the template presence, and then its absence after extraction. Figure S1 shows the spectra recorded for the MIP and NIP films before and after template extraction. The PQQPFPQQ-entrapped MIP film shows bands in the region of 1445–1480 cm^{-1} corresponding to antisymmetric bending vibration of the CH_3 substituent, typical for phenylalanine in proteins.[36] Moreover, the ~1659 cm^{-1} band is seen in the spectrum of the MIP before extraction. This band is typical for the stretching C=O vibration in proteins containing glutamine (curve *1* in Figure S1 in Supporting Information).[36] Relative intensity of these bands decreased after PQQPFPQQ template extraction (curve *2* in Figure S1 in Supporting Information).

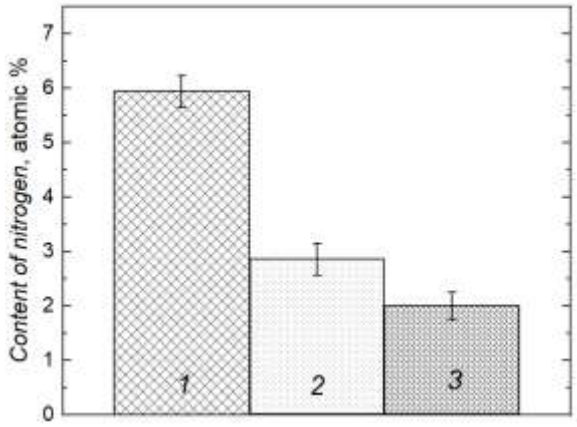

Figure 2. Histograms comparing the nitrogen content, obtained with high-resolution XPS, for the MIP film (*1*) before PQQPFPQQ template extraction, (*2*) after PQQPFPQQ template extraction with the 10-mM NaOH and ethanol mixture at the volume ratio of 1 : 2 (*v* : *v*), for 3 h, and (*3*) for the NIP film.

The surface of the imprinted and non-imprinted polymer films was characterized by AFM imaging (Figure 3). That is, MIP and NIP films were imaged before and after template extraction. Apparently, the MIP film before extraction was relatively rough being composed of clusters smaller than those of the NIP film. The NIP film was much thicker and rougher than the MIP film was. Treatment of both films with the extraction solution increased their roughness. Moreover, nanomechanical properties (Young's modulus, adhesion, deformation, and dissipation) of the films were unraveled (Figures S2-S6 in Supporting Information). The determined values of these parameters are presented in Table S2 in Supporting Information.

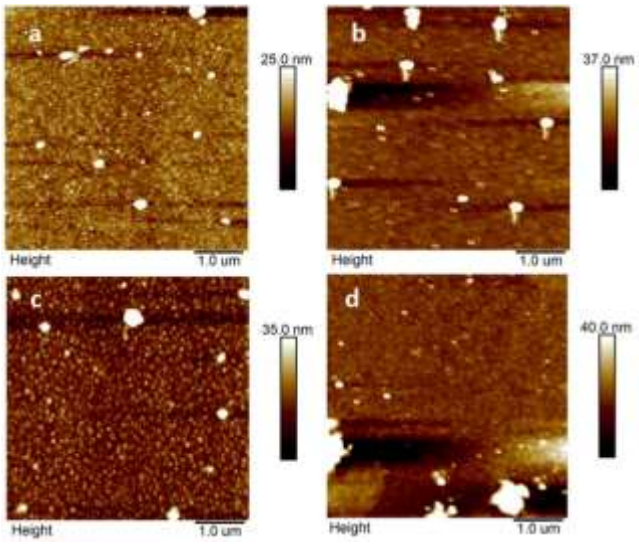

Figure 3. Semi-contact atomic force microscopy (1×1 μm^2) images of the PQQPFPQQ-templated MIP film (a) before and (b) after extraction of the PQQPFPQQ template as well as for the NIP film (c) before and (d) after treatment same as that used for template extraction from MIP film. Results of more extensive AFM study are shown in Figures S2-S6 in Supporting Information.

Table 2. Parameters of the MIP and NIP films determined by AFM before and after template extraction.

Sample	Roughness, nm	Thickness, nm
MIP		
as prepared	2.1 ± 0.3	161 ± 4
after PQQPFPQQ template extraction	4.0 ± 1.9	149 ± 3
NIP		
as prepared	3.4 ± 0.7	202 ± 17
after washing	4.6 ± 3.5	203 ± 13

EG-FET measurements

After template extraction, the PQQPFPQQ analyte binding by vacated imprinted cavities of MIP was examined. For the determination of this binding, electrical transduction with the EG-FET was used.

When a positive with respect to the source of the n-type channel MOSFET voltage is applied to the gate, electrons, which are the major charge carriers in the heterostructure, are attracted to the surface of the gate forming a conducting channel between the source and the drain.[31,37] Accordingly, the transistor characteristics were measured at the constant gate voltage of 1.50 V applied while the drain voltage (V_D) was scanned from 0 to 5.0 V, and the change in the resulting drain current (I_D) was measured. The I_D changes, recorded for different concentrations of the PQQPFPQQ analyte, allowed monitoring the extent of the analyte molecules binding by imprinted molecular cavities from 0.5 mM MES buffer (pH=6.2).

The dependence of the change in the drain current (ΔI_D) on the PQQPFPQQ concentration change with time, as determined from the EG-FET characteristics (Figure S7 in Supporting Information), was attributed to the interfacial potential change at the (extended gate)-solution interface. The EG-FET chemosensor limit of detection of the PQQPFPQQ epitope was lower than 4 ppm, which is the gluten detectability demanded in commercial gluten sensing kits.[38]

As expected for successful imprinting, the isotherm for the binding of the PQQPFPQQ template to the MIP cavities showed a saturation course (Figure 4). Within the considered concentration range of ~2 orders of magnitude, the ΔI_D was linearly dependent on the logarithm of the analyte concentration in solution (Figure 5).

To estimate MIP selectivity, the slope of the calibration plot for the PQQPFPQQ analyte and that for the PQQ**Q**FP**P**Q interferent, at the MIP-PQQPFPQQ, were compared. It appeared that the MIP-PQQPFPQQ chemosensor response to the PQQPFPQQ analyte (curve *1* in Figure 4) was much higher than that to the PQQ**Q**FP**P**Q interferent (with two mismatched amino acids), thus resulting in the selectivity of molecular recognition in the MIP film as high as ~125. This favorable behavior most likely arises from the presence of highly selective molecular cavities generated during the imprinting. Table 3 summarizes analytical parameters determined for the MIP chemosensor devised.

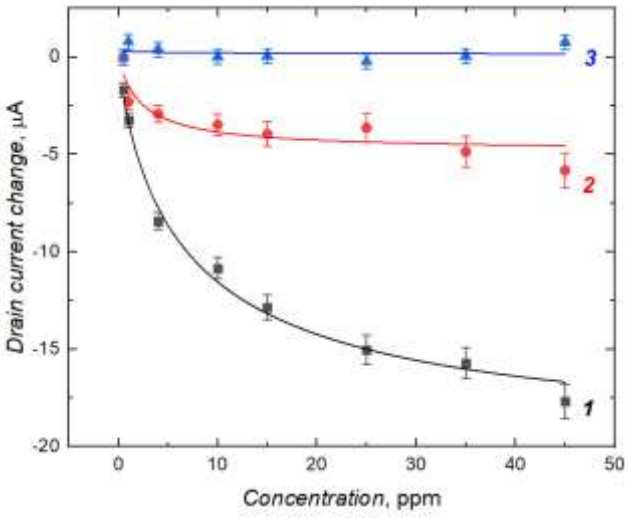

Figure 4. The drain current change dependence for the EG-FET chemosensor with its gate coated with the MIP-PQQPFPQQ film on the concentration of (curve *1*) the PQQPFPQQ analyte and (curve *3*) the PQQ**Q**FP**P**Q interferent as well as (curve *2*) the PQQPFPQQ analyte for the EG-FET chemosensor with its gate coated with the NIP film. The extended-gate surface area was ~ 21 mm^2. The applied gate voltage was, V_G = 1.5 V.

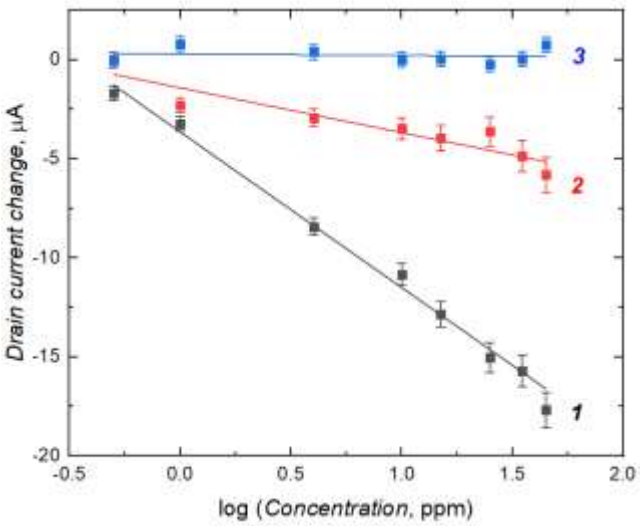

Figure 5. Calibration plots for the EG-FET chemosensor with its gate coated with the MIP-PQQPFPQQ film for (curve *1*) the PQQPFPQQ analyte and (curve *3*) the PQQ**Q**FP**P**Q interferent as well as for (curve *2*) the EG-FET chemosensor with its gate coated with the NIP film for the PQQPFPQQ analyte. The extended-gate surface area was ~ 21 mm^2. The applied gate voltage was, V_G = 1.5 V.

Table 3. Analytical parameters of the devised MIP based EG-FET chemosensor for determination of the PQQPFPQQ gluten epitope.

Recognition unit	Analytical parameter	Value±st.dev.
MIP	Sensitivity to PQQPFPQQ, μA ppm^{-1}	8.06±0.29
	Linear dynamic concentration range, ppm	0.5–45
	Limit of detection at 3σ, ppm	0.11
	Sensitivity to PQQ**Q**FP**P**Q, μA ppm^{-1}	0.06±0.21
NIP	Sensitivity to PQQPFPQQ, μA ppm^{-1}	1.92±0.43

In order to confirm the imprinting, an NIP film deposited on the Au-glass slide electrode was assembled in the EG-FET system. Because of the absence of molecular cavities, PQQPFPQQ binding to the NIP was weaker than to the MIP (curve *2* in Figure 4). The sensitivity of the NIP electrode to PQQPFPQQ was much lower than that of the MIP electrode (Table 3). The apparent imprinting factor (AIF),[33] was determined from the ratio of slopes of calibration curves for the MIP and NIP of EG-FET chemosensors, was as high as, AIF = 4.2.

Gluten determination in real samples with the (EG-FET)-MIP chemosensor

The analytical response of the (EG-FET)-MIP chemosensor was validated with respect to a real sample of the gluten

extract from semolina flour. The chemosensor was very sensitive to the gluten content in this extract (Figures S9b and S10b in Supporting Information). Moreover, the chemosensor response to gluten from semolina was quasi-linear in the concentration range of 0.5 to 15 ppm of gluten, which is similar to the range of the response of immuno-based commercial gluten test. Figure 6 correlates gluten determination in semolina flour by the (EG-FET)-MIP and ELISA. A high correlation obtained (R^2 = 0.980) indicates that our proposed new EG-FET involving method of gluten determination in flour samples is both reliable and comparable with that performed using a commercially available gluten kit.

Sorption models fitting

The Langmuir,[39] Freundlich,[40] and Langmuir-Freundlich[41] (Figures 5 and S8-S10 as well as Tables S3-S5 in Supporting Information) isotherms were fitted to the peptide sorption experimental data of PQQPFPQQ and real samples determined using two different procedures, i.e., one involving the (EG-FET)-MIP and the other the ELISA test. Apparently, the Langmuir and Langmuir-Freundlich isotherms best fitted to the experimental PQQPFPQQ sorption data with equal correlation coefficients, R^2 = 0.992. Therefore, the imprinted cavities were quite homogenous with the heterogeneity index, m = 0.75 ± 0.11. This heterogeneity index varies in the range of $0 \leq m \leq 1$; m approaches 1 as heterogenity decreases and equals 1 for a homogeneous system. Density of imprinted cavities, N, was similar in both of these models. That is, its absolute value was 19 and 22 for the Langmuir and the Langmuir-Freundlich isotherm, respectively. This result can indicate that each epitope molecule occupies just one imprinted cavity and the sorption nature is chemical. After all molecular cavities are occupied by analyte molecules, the analyte is then physisorbed by the polymer network.

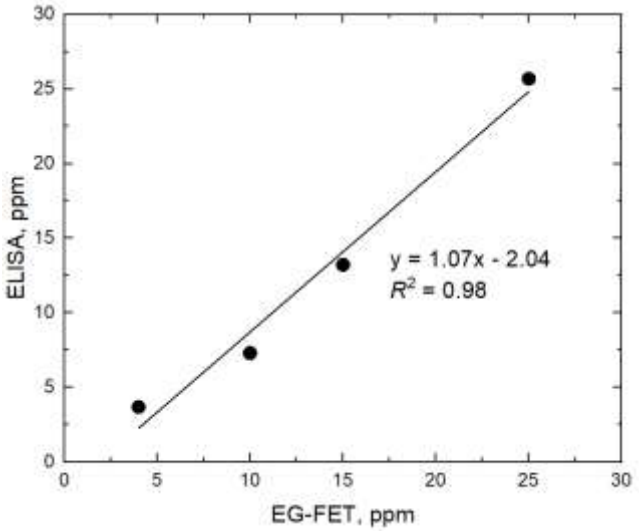

Figure 6. Correlation of the (EG-FET)-MIP and ELISA determined gluten content in semolina flour.

Conclusions

We devised and fabricated a new (EG-FET)-MIP based chemosensor using a thin film of an MIP imprinted with the PQQPFPQQ gluten epitope as the recognition unit for selective epitope analyte determination. This film was deposited by electropolymerization on surface of the extended gate of the field-effect transistor. The resulting chemosensor successfully determined the PQQPFPQQ gluten epitope in the concentration range of 0.5 to 45 ppm with the limit of detection of 0.11 ppm PQQPFPQQ and a very high selectivity with respect to the PQQ**Q**FP**P**Q interferent bearing only 2 mismatched amino acids. The calculated value of the apparent imprinting factor was, AIF = 4.2, thus indicating a high concentration of imprinted molecular cavities in the MIP selective to molecules of the PQQPFPQQ gluten epitope. Moreover, the chemosensor was capable of determining gluten in real samples of semolina flour. Performance of our new method using the (EG-FET)-MIP chemosensor was comparable to that of the ELISA sensing system. Both Langmuir and Langmuir-Freundlich models equally well fitted to the experimental epitope sorption data indicating that the imprinted cavities were quite homogenous and the epitope analyte was chemisorbed in these cavities.

Although the herein presented results are encouraging, the chemosensor needs to be further tested on a large variety of real samples.

ASSOCIATED CONTENT

Supporting Information

The Supporting Information is available free of charge on the ACS Publications website.

Information on the gluten epitope PQQPFPQQ (Scheme S1). Information on pre-polymerization complex formation with different functional monomers (Scheme S2 and Table S1). Information on polarization-modulation infrared reflection-absorption spectroscopy, PM-IRRAS (Figure S1). Information on atomic force microscopy, AFM, study (Figures S2-S6 and Table S2). Information on chemosensor validation (Figure S7). Information on the Romer Labs® ELISA gluten kit. Information on the sorption model fitting (Figures S8-S10 and Tables S3-S5).

AUTHOR INFORMATION

Corresponding Author

* zofiaewa.iskierko@univr.it;
* wkutner@ichf.edu.pl;
* alessandramaria.bossi@univr.it;

Present Addresses

[1]Department of Biotechnology, University of Verona, Strada Le Grazie 15, 37134 Verona, Italy

[2]Institute of Physical Chemistry, Polish Academy of Sciences (IPC PAS), Kasprzaka 44/52, 01-224 Warsaw, Poland

[3]Faculty of Mathematics and Natural Sciences, School of Sciences, Cardinal Stefan Wyszynski University in Warsaw

Author Contributions

The manuscript was written through contributions of all authors. All authors have given approval to the final version of the manuscript.

ACKNOWLEDGMENT

The present research was financed by the Polish Science Centre, NCN through Grant No. 2013/11/N/ST5/01907, the Foundation for Polish Science (FNP, START 23.2017).

AMB and ZI acknowledge the European Union's Horizon 2020 research and innovation programme under the Marie Sklodowska-Curie grant agreement GEMS No. 752438 for supporting in part the present work.

W.K. acknowledges financial support from National Science Center of Poland, NCN, through Grant No. 2014/15/B/NZ7/01011.

We thank Prof. Tiziana Benincori (Department of Chemical and Environmental Sciences, University of Insubria, Como, Italy) and Prof. Francis D'Souza (Department of Chemistry, University of North Texas, Denton) for synthesizing the cross-linking monomer and functional monomers, respectively.

REFERENCES

(1) Long, K. H.; Rubio-Tapia, A.; Wagie, A. E.; 3rd, L. J. M.; Lahr, B. D.; Dyke, C. T. V.; Murray, J. A. *Aliment. Pharmacol. Ther.* **2010**, *32*, 261.
(2) Scherf, K. A.; Wieser, H.; Koehler, P. *Food Res. Int.* **2018**, *110*, 62-72.
(3) Schuppan, D. *Gastroenterology* **2000**, *119*, 234-242.
(4) Schalk, K.; Lang, C.; Wieser, H.; Koehler, P.; Scherf, K. A. *Nat. Sci. Rep.* **2017**, *7*, 45092.
(5) Eksin E.; Congur G.; Erdem A.. *Food Chem.* **2015**, *184*, 183–187.
(6) Erdem A.; Papakonstantinou P.; Murphy H.. *Anal. Chem.* **2006**, *18*, 6656–6659.
(7) Shewry, P. R.; Halford, N. G.; Belton, P. S.; Tatham, A. S. *Phil. Trans. R. Soc. Lond. B* **2002**, *357*, 133–142.
(8) Wieser, H. *Food Microbiol.* **2007**, *24*, 115–119.
(9) Sollid, L. M.; Qiao, S.-W.; Anderson, R. P.; Gianfrani, C.; Koning, F. *Immunogenetic* **2012**, *64*, 455–460.
(10) Angelis, M. D.; Cassone, A.; Rizzello, C. G.; Gagliardi, F.; Minervini, F.; Calasso, M.; Cagno, R. D.; Francavilla, R.; Gobbetti, M. *Appl. Environ. Microbiol.* **2010**, *76*, 508-518.
(11) Shan, L.; Molberg, Ø.; Parrot, I.; Hausch, F.; Filiz, F.; Gray, G. M.; Sollid, L. M.; Khosla, C. *Science* **2002**, *297*, 2275-2279.
(12) Waga, J.; Skoczkowski, A. *Euphytica* **2014**, *195*, 105–116.
(13) Tatham, A. S.; Shewry, P. R. *J. Cereal Sci.* **1995**, *22*, 1-16.
(14) Ensari, A.; Marsh, M. N.; Moriarty, K. J.; Moore, C. M.; Fido, R. J.; Tatham, A. S. *Clin. Sci.* **1998**, *95*, 419–424.
(15) Sharma, P. S.; D'Souza, F.; Kutner, W. *TrAC-Trends Anal. Chem.* **2012**, *34*, 59-77.
(16) Wulff, G. *Chem. Rev.* **2002**, *102*, 1-28.
(17) Sharma, P. S.; Pietrzyk-Le, A.; D'Souza, F.; Kutner, W. *Anal. Bioanal. Chem.* **2012**, *402*, 3177–3204.
(18) Suriyanarayanan, S.; Cywinski, P. J.; Moro, A. J.; Mohr, G. J.; Kutner, W. *Top. Curr. Chem.* **2012**, *325*, 165–266.
(19) Malitesta, C.; Mazzotta, E.; Picca, R. A.; Poma, A.; Chianella, I.; Piletsky, S. A. *Anal. Bioanal. Chem.* **2012**, *402*, 1827–1846.
(20) Wackerlig, J.; Lieberzeit, P. A. *Sens. Actuators, B* **2015**, *207*, 144-157.
(21) Alexander, C.; Andersson, H. S.; Andersson, L. I.; Ansell, R. J.; Kirsch, N.; Nicholls, I. A.; O'Mahony, J.; Whitcombe, M. J. *J. Mol. Recognit.* **2006**, *19*, 106-180.
(22) Whitcombe, M. J.; Kirsch, N.; Nicholls, I. A. *J. Mol. Recognit.* **2014**, *27*, 297–401.
(23) Rachkov, A.; Minoura, N. *Biochim. Biophys. Acta; - Protein Structure and Molecular Enzymology* **2001**, *1544*, 255-266.
(24) Nishino, H.; Huang, C. S.; Shea, K. J. *Angew. Chem. Int. Ed. Engl.* **2006**, *45*, 2392-2396.
(25) Bertolla, M.; Cenci, L.; Anesi, A.; Ambrosi, E.; Tagliaro, F.; Vanzetti, L.; Guella, G.; Bossi, A. M. *ACS Appl. Mater. Interfaces* **2017**, *9*.
(26) Iskierko, Z.; Noworyta, K.; Sharma, P. S. *Biosens. Bioelectron.* **2018**, *109*, 50–62.
(27) Huynh, T.-P.; Bikram, K. C.; Lisowski, W.; D'Souza, F.; Kutner, W. *Bioelectrochemistry* **2013**, *93*, 37–45.
(28) Pietrzyk, A.; Suriyanarayanan, S.; Kutner, W.; Zandler, M. E.; D'Souza, F. *Bioelectrochemistry* **2010**, *80*, 62–72.
(29) Sannicolo, F.; Mussini, P. R.; Benincori, T.; Martinazzo, R.; Arnaboldi, S.; Appoloni, G.; Panigati, M.; Procopio, E. Q.; Marino, V.; Cirilli, R.; Casolo, S.; Kutner, W.; Noworyta, K.; Pietrzyk-Le, A.; Iskierko, Z.; Bartold, K. *Chem. Eur. J.* **2016**, *22*, 10839 – 10847.
(30) Frisch M. J.; et al. *Gaussian, Inc.: Wallingford CT,* **2009**.
(31) Iskierko, Z.; Sosnowska, M.; Sharma, P. S.; Benincori, T.; D'Souza, F.; Kaminska, I.; Fronc, K.; Noworyta, K. *Biosens. Bioelectron.* **2015**, *74*, 526–533.
(32) Iskierko, Z.; Sharma, P. S.; Prochowicz, D.; Fronc, K.; D'Souza, F.; Toczydłowska, D.; Stefaniak, F.; Noworyta, K. *ACS Appl. Mater. Interfaces* **2016**, *8*, 19860–19865.
(33) Iskierko, Z.; Checinska, A.; Sharma, P. S.; Golebiewska, K.; Noworyta, K.; Borowicz, P.; Fronc, K.; Bandi, V.; D'Souza, F.; Kutner, W. *J. Mater. Chem. C* **2017**, *5*, 969-977.
(34) Jamroz, M. H. *Institute of Nuclear Chemistry and Technology, Warsaw, Poland* **2014**, *SPESCA, Spectroscopy and molecular modeling group*.
(35) Heinze, J.; Frontana-Uribe, B. A.; Ludwigs, S. *Chem. Rev.* **2010**, *110*, 4724–4771.
(36) Barth, A. *Prog. Biophys. Mol. Biol.* **2000**, *74*, 141-173.
(37) Dabrowski, M.; Sharma, P. S.; Iskierko, Z.; Noworyta, K.; Cieplak, M.; Lisowski, W.; Oborska, S.; Kuhn, A.; Kutner, W. *Biosens. Bioelectron.* **2016**, *79*, 627–635.
(38)https://www.romerlabs.com/en/analytes/food-allergens/gluten-test-kits/.
(39) Yang, H.; Nishitani, S.; Sakata, T. *ECS J. Solid State Sci. Technol.* **2018**, *7*, Q3079-Q3082.
(40) UmplebyII, R. J.; Baxter, S. C.; Bode, M.; Jr., J. K. B.; Shah, R. N.; Shimizu, K. D. *Anal. Chim. Acta* **2001**, *435*, 35–42.
(41) UmplebyII, R. J.; Baxter, S. C.; Chen, Y.; Shah, R. N.; Shimizu, K. D. *Anal. Chem.* **2001**, *73*, 4584–4591.

TOC graphics for Table of Contents only